JMEPEG (2010) 19:401–412
DOI: 10.1007/s11665-009-9495-6

1059-9495/$19.00

Nitriding of Aluminum Extrusion Die: Effect of Die Geometry

S.S. Akhtar, A.F.M. Arif, and B.S. Yilbas

(Submitted December 26, 2008; in revised form March 5, 2009)

Nitriding of complex-shaped extrusion dies may result in non-uniform nitride layers and hence a required hardness may not be achieved in some regions of the bearing area. The present study is carried out to assess the effect of extrusion die profile on the characteristics and growth behavior of nitride layers so that the critical die design feature can be identified to enhance the uniformity of the nitride layer. For this purpose, AISI H13 steel samples have been manufactured with profiles similar to those of hot extrusion dies. The samples were then gas nitrided under controlled nitriding potential. The uniformity and depth of nitride layers have been investigated in terms of compound layer and total nitride case depth for selected die features. The results of this study indicated the need to include the effect of profile on the nitride layer for the optimal die design with improved service life.

Keywords AISI H13 extrusion die, gas nitriding, metallurgical study, profile geometry

1. Introduction

Although gas nitriding of extrusion dies and other steel components is well established surface hardening treatment, several aspects of the nitride layers still require attention and research. An important issue arises from the fact that extrusion dies of H13 tool steel for the production of aluminum profiles involve very complex shapes. To improve the nitriding uniformity, it is important to identify critical geometric features in the die with respect to nitriding layer formation. Corrective action in the controlled nitriding process then may be incorporated accordingly.

The detailed systematic work has not been found in the open literature investigating the nitride layer growth around die profiles with intricate geometric features. Kwon et al. (Ref 1) study the growth behavior of the nitrided layer inside a Cr-Mo steel hollow tube with corrugation over the internal surface. They observed differences in the compound and nitrided layer thicknesses on the land and groove surfaces and their dependence on the size of geometric features. Non-uniformity in the nitrided layer thickness and variation with size and shape of the test specimen during plasma nitriding was reported by Ataide et al. (Ref 2). Alves et al. (Ref 3) studied the growth behavior of plasma-nitrided layers on AISI 316 stainless work pieces with complex geometry. They found significant differences in thickness and hardness of the resulting nitrided layers as a function of nitriding parameters. The observed thickness of nitrided layers increased with sample height. Tercelj et al. (Ref 4) studied the ionic and gas nitriding of dies made of H10 tool steel with narrow and deep gaps. A similar type of study was carried out by Kugler et al. (Ref 5) for AISI H13 dies. In both studies, variation in the nitriding depth and compound layer thickness with varying gap sizes were observed. Nayal et al. (Ref 6) presented a comparison of pulse-plasma-nitrided flat coupons and complex-shaped substrates such as twist drill test bits and showed that the incorporation of nitrogen depends strongly on the substrate geometry. They showed that the amount of nitrogen incorporated at the cutting edge of a drill was systematically higher than in flat coupons nitrided under identical plasma conditions. Reinhold et al. (Ref 7) carried out plasma nitriding on various aluminum alloys to study the formation of aluminum nitride layers in dependence on the chemical composition and geometry. Besides simple flat specimens, more complex-shaped samples were investigated to get information about the uniformity of film covering.

In the present study, the geometric features commonly used in the design of aluminum extrusion profiles have been considered to investigate the effect of geometric features on the nitriding characteristics of the AISI H13 steel. Different extrusion die profiles were collected from local extrusion plant and some most commonly used profiles were modeled using Solid-Works code. The profiles were cut in H13 blanks with CNC wire electro-discharge machine (EDM) in collaboration with local extrusion die manufacturing setup. All the samples were nitrided using two-stage controlled gas nitriding process.

2. Experimental

2.1 Samples Preparation

Different extrusion die profile drawings were collected from local extrusion plant to prepare the samples. The purpose of using actual die profiles is to resemble the real industrial dies to investigate the effect of die geometric complexity on the resulting nitride layer. Some of the representative collected profiles incorporated in the samples are shown in Fig. 1. It

S.S. Akhtar, A.F.M. Arif, and **B.S. Yilbas**, Mechanical Engineering Department, King Fahd University of Petroleum & Minerals, Dhahran, Saudi Arabia. Contact e-mail: bsyilbas@kfupm.edu.sa.

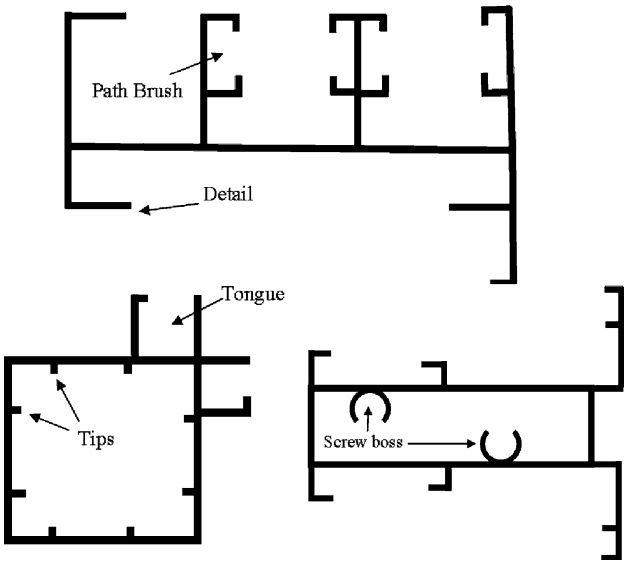

Fig. 1 Representative profile drawings used in the study

should be noted that these three extrusion profiles are representative, which are selected from about 150 die profile drawings collected from local extrusion industry. The five features, namely screw boss, path brush, tongue, details, and tips, are the most common and usually present in almost every complex die. Three samples were prepared by incorporating the most common and frequently used profiles as shown in Fig. 2. Both dimensional drawings and actual samples are shown. It can be observed from Fig. 2 that three different details (D-1, D-2, and D-3) and two tip types (T-1 and T-2) are included in the study. CNC wire EDM was used to produce the samples. The thickness of the samples was kept at 5 mm. The material of samples is H13 tool steel (commercial name: ORVAR 2 Microdized), a typical die steel used for hot extrusion dies having composition (wt.%): 0.39% C, 1% Si, 0.4% Mn, 5.3% Cr, 1.9% Mo, 0.9% V and balance Fe. The samples were heat treated with proper environmental control using vacuum furnace to prevent decarburization. The heat-treatment cycle included stress relieving at 650 °C, pre-heating at 815 °C, austenitizing at 1030 °C, quenching, and finally double tempering (first at 550 °C and second at 650 °C). After first tempering, the

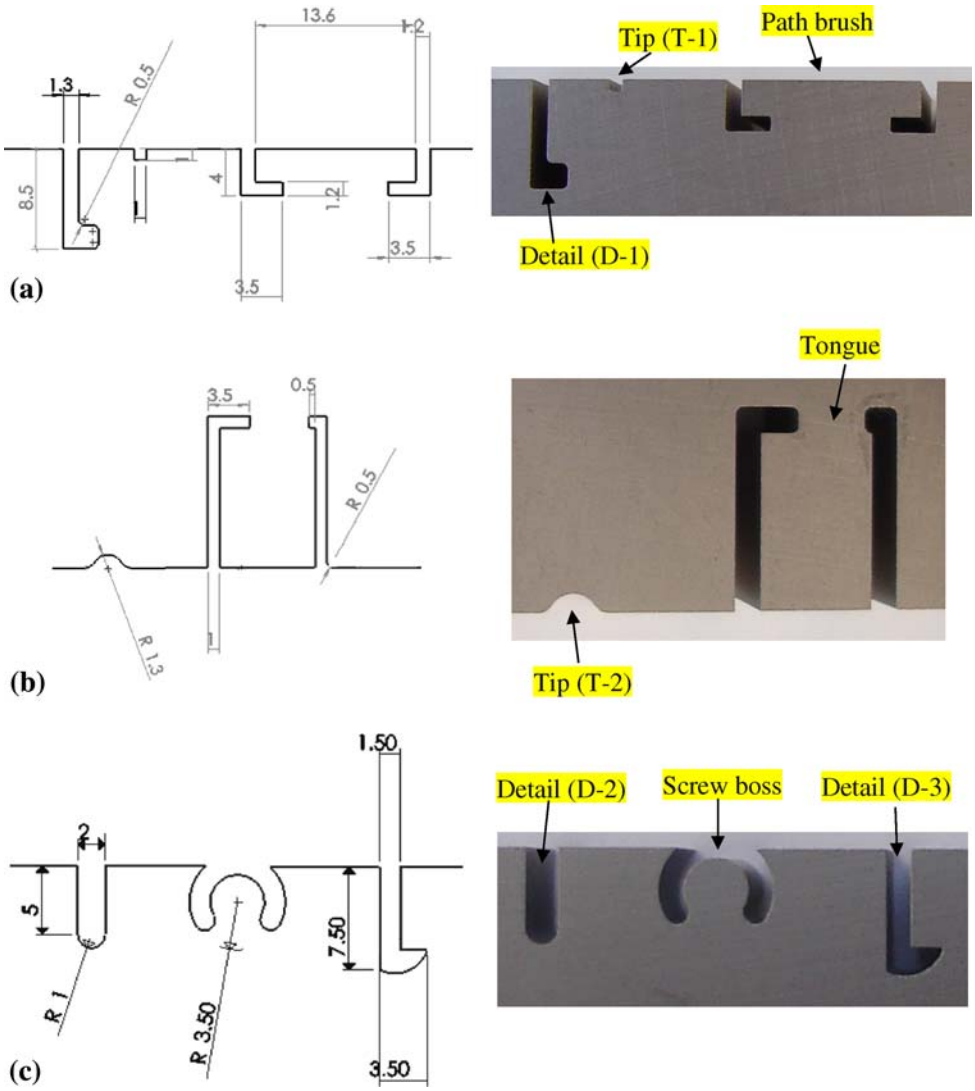

Fig. 2 Dimensional drawings and actual samples (all dimensions are in millimeters). Studied profiles are highlighted

expected embrittling effects of coarse carbide structure, formed by the transformation of retained austenite to tempered martensite, were alleviated by subsequent second tempering.

2.2 Nitriding Cycle Used for Samples

The samples were gas nitrided using two-stage nitriding process with controlled nitriding potential in collaboration with local extrusion setup. Equipment with a trade name Nitreg® developed by NITREX Metal Inc. was employed for this purpose. The nitriding furnace is shown in Fig. 3, which is the top-loading design with a swing type cover, available with a selection of options to meet process requirements, and capable of handling a wide range of applications and work piece sizes. This nitriding system was capable of maintaining the pre-set values of nitriding potential ($K_n = p_{NH_3}/(p_{H_2})^{3/2}$, where p is the partial pressure of constituting gas). The values of nitriding potentials (K_n) were maintained within certain limits as desired for each processing stage by continuous self-correction. The system set the flows for nitrogen and ammonia according to the pre-set program. Figure 4(a) shows the variations of temperature and gas flow rate in the furnace during the nitriding cycle. The operating nitriding temperatures for stage 1 and stage 2 were 490 and 530 °C, respectively. Set-point K_n values of 6.4 $(atm)^{-1/2}$ and 0.323 $(atm)^{-1/2}$ were used for stage 1 and stage 2, respectively. The furnace was first preheated and equalized to the preset temperature (450 °C) for about 3 h. The air in the retort was replaced by the ammonia and nitrogen gas mixture. The filling time (1 h and 40 min) was calculated automatically by the control system, based on the furnace volume and incoming gas flow. During each process stage, the temperature and gas flow were controlled to achieve the set-point K_n values, which depends upon ammonia dissociation percentage. The in-process variation of K_n during the nitriding cycle is shown in Fig. 4(b), recorded at an interval of 10 min. Such K_n variation depicts a decrease of ammonia percentage from stage 1 to stage 2 (i.e., an atmosphere with increased dissociation of ammonia from stage 1 to stage 2). The heat stages were activated automatically, before the next process stage commences. The time of heating 1 and heating 2 prior to stage 1 and stage 2, respectively, was set to 1 h. The processing time for stages 1 and 2 was 1.5 and 3.3 h, respectively. The total nitriding cycle took about 15 h; however, the actual nitriding time was about 6.8 h corresponding to heating 1 through stage 2 as illustrated in Fig. 4(a). It should be noted that through adjustment of the retort (i.e., K_n), it is possible to form compound layer of the required phase composition and required thickness. The thickness and phase structure of the compound layer considerably affect the die performance. For extrusion dies, a deep case is not required; a shallow case will be sufficient to the maximum of 250 μm, with formation of compound layer in the region of 10% of the total case depth. The surface may begin to lose its flexibility with a deep case formation, which may lead to surface cracking and thus early die maintenance resulting in press downtime. The recommended ranges K_n values and maximum allowed thickness of compound layer for different classes as classified by Aerospace Material Specification (AMS) per requirement of AMS 2759/10A (Ref 8) are given in Table 1. The same recommended ranges of K_n were adopted in the present study.

Fig. 3 Nitriding furnace, a top-loading design with a swing type cover (a) a "drain" of furnace for samples (b); process control hardware including process control, gas and electrical panels (c). Courtesy: Aluminum Products company, Dammam, Saudi Arabia

2.3 Samples Preparation and Microscopic Examination of Nitride Layers

Five die profiles for the most common extruded sections in the extrusion industry were carefully selected, which are given in Table 2. These are also identified in actual die profile drawings (Fig. 1). The five profiles are in accordance with a previous study (Ref 9):

(a) *Screw boss*: used later for fastening the extruded section to a structure
(b) *Path brush*: slotted groove on which a rubber lining is later fitted
(c) *Tongue*: a partially open rectangular extension, usually attached to a hollow profile
(d) *Details*: small appendages to the main profile, in effect minor sub-profiles
(e) *Tips*: a very small protrusion, either sharp or rounded

These profiles encompass some of the very common features which are included in the study. These features have been divided into five categories as following.

(a) Curved-convex surface (CX)
(b) Curved-concave surface (CV)
(c) Corner inner (CI)
(d) Corner outer (CO)
(e) Flat surface (F)

As can be observed from Table 2, a total of 15 features from the aforementioned five profiles have been selected including three from each category of features.

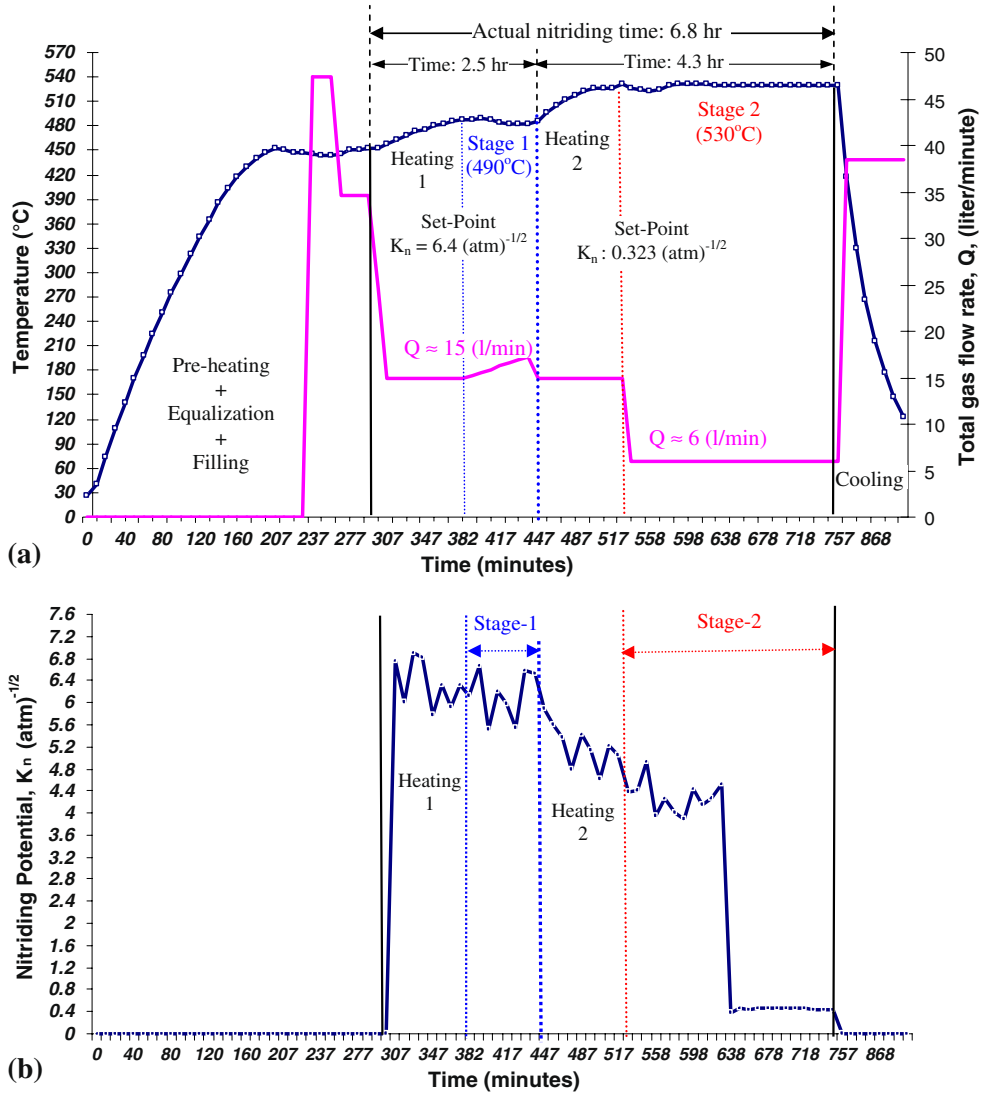

Fig. 4 In-process variations of temperature (a) and nitriding potential, K_n (b) during two-stage nitriding of AISI H13 samples having different geometric profiles

Table 1 AMS recommended ranges of nitriding potential and thickness of compound layer in two-stage controlled gaseous nitriding of H11/H13 steel

	Class 1		Class 2	
Process stage:	**Stage 1**	**Stage 2**	**Stage 1**	**Stage 2**
K_n (atm)$^{-1/2}$	5-15	0.4-0.9	5-15	2.2-5.5
Maximum compound layer	13 μm		25 μm	

For the sectioning of sample to cross section, CHMER CNC wire EDM was used. After cutting the samples, they were ground and polished with diamond paste (initially with 3 μm and finally with 0.25 μm) and etched with nital (1 vol.% HNO_3 in ethyl alcohol) for about 7 s prior to examination. The cross sections were investigated using Axioplan 2 imaging optical microscope. The SEM micrographs were analyzed with Jeol JSM-6460LV scanning electron microscope. The microhardness measurements were performed across the cross sections of the nitrided specimens using BUEHLER Wirtz apparatus under an applied load of 300 g.

3. Results and Discussion

Metallographic investigations were performed using optical and scanning electronic microscopes followed by microhardness measurement to observe the nitride layer formation and its uniformity on 15 different features encompassed by the most common die profiles. The optical and scanning electron microstructures of the nitride cross sections of all 15 features with corresponding hardness depth profiles are shown in Fig. 5 to 14.

It can be observed that all microstructures consist of a nitride layer at the external surface. The nitride layer consists of a diffusion zone with fine nitride precipitates (dark regions in the optical and lamellae structure in the SEM micrographs) with or without a compound layer at the surface. It can be observed that the compound zone is more visible in SEM micrographs than

Table 2 Selected die profiles and geometric features

Die profiles for some common extruded sections used in the study
Screw boss
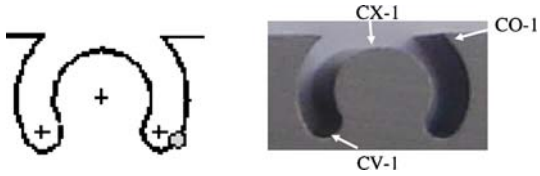
Path brush
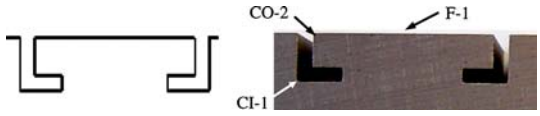
Tongue

Details
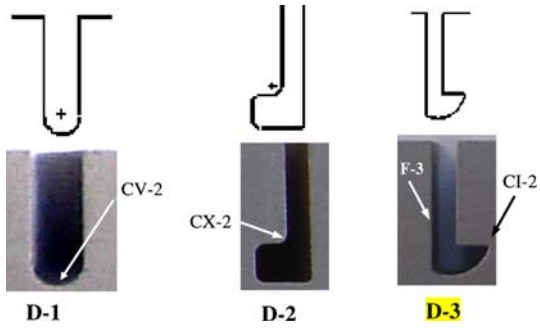
Tips
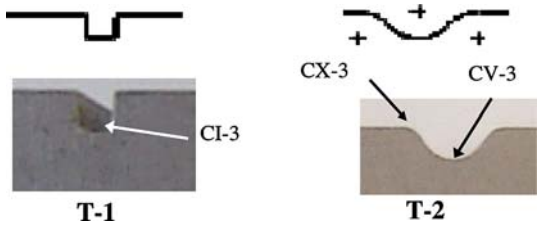

the optical micrographs due to the optical reflection of the surface. The thickness of compound layer at each feature location is estimated from the corresponding SEM micrograph and is listed in Table 3.

The Lehrer's equilibrium diagram (as shown in Fig. 15) illustrates the relationship between nitriding potential (K_n), the nitriding temperature and the phases α, γ′ and ε in equilibrium. This diagram can be used to observe the effect of nitriding potential on the formation of the ε or γ′ phases in the surface region. It is assumed that the shifts in the Lehrer diagram caused by alloying elements are not large and can be used for H13 steel. The critical nitriding potential values and hence the nitrogen activities above which the iron nitrides in the compound layer ($\gamma' - Fe_4N$ and $\varepsilon - Fe_3N$) develop can be identified. The actual variation of K_n (Fig. 4b), also indicates that the compound layer would form at the surface. It is evident from Lehrer equilibrium diagram that the $\gamma' - Fe_4N$ phase of compound layer begins to form when K_n of the atmosphere exceeds the upper limit of nitrogen concentration in the α zone (diffusion zone) at nitriding temperature. Further increase of K_n causes the formation of the ε phase on the steel surface. The recommended ranges K_n values and maximum allowed thickness of compound layer for different classes as classified by AMS per requirement of AMS 2759/10A were used. Moreover, the thickness of the compound layer achieved in all 15 features is less than the maximum specified by AMS.

The hardness measurements were taken at a specific location (depth) starting from about 10 μm away from the surface. Each indentation point in the hardness-depth profiles is the result of average of five measurements at each location. It can be seen that the pattern of hardness depth profile is the same for all features, maximum near the surface and decays toward the core of material. However, the hardness profile along the depth varies despite the fact that the samples are made of the same material and nitrided under same conditions. The core hardness was measured as 660 HV for the locations. The nitrided depth at each feature location is determined from hardness-depth profile using the criteria that depth below the surface at which micro-hardness is 10% higher than that of the core (Ref 8). The nitrided depth at each location is given in Table 3.

The influence of surface texture on the nitriding process is described in the subsequent sections.

3.1 Flat-Surface Feature

Almost uniform and similar nitride layers are achieved at the locations selected for examinations as shown in the optical and scanning electron micrographs (Fig. 5). Moreover, the compound layer on the order of 4 μm is achieved as desired for extrusion dies. It can be observed from the case depth developed for feature F-3 (corresponding to profile *detail D-3*) that surface location and orientation play an important part in controlling the case formation. A comparatively small nitrided depth for F-3 can be attributed to relatively indirect access of nitrogen during diffusion as compared to other two flat surfaces. Comparing hardness profiles for the flat surfaces (Fig. 6), F-1 has the highest maximum-hardness on the order of 1300 HV with monotonic decrease toward the core material. However, the other flat surfaces have the maximum-hardness in the range of 1150 HV. It shows that F-1 corresponding to *path brush*, which has more direct exposure to the nitrogen resulted in satisfactory nitride layer. The same reason is also valid for uniform and slightly thick compound layer in the case of F-1.

3.2 Corner-Outer Feature

This results in deep nitride case depth as shown in Fig. 7. This is due to simultaneous diffusion from two convergent directions at the corners. The compound layer thickness is the least for these features as shown in Table 3 and can be observed from the corresponding SEM micrographs (Fig. 7). The hardness curves for corner-outer feature locations (Fig. 8) are relatively less steep and having deeper hardening effect in line

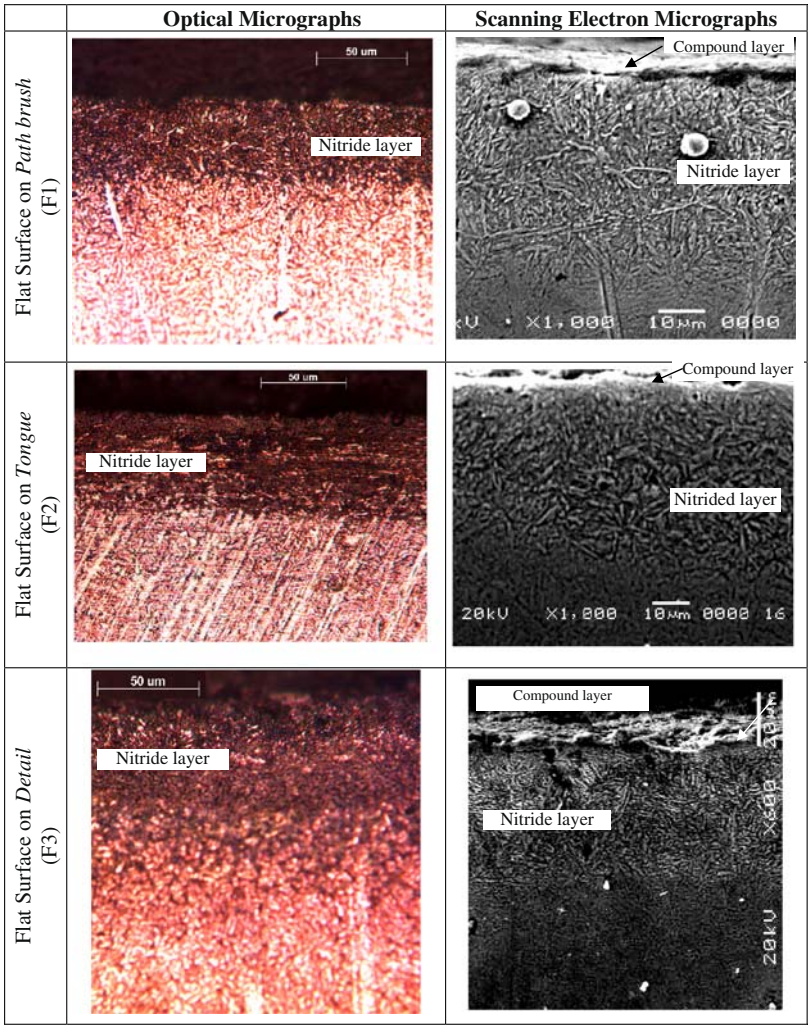

Fig. 5 Optical and scanning electron micrographs of nitrided cross-sections observed at flat features

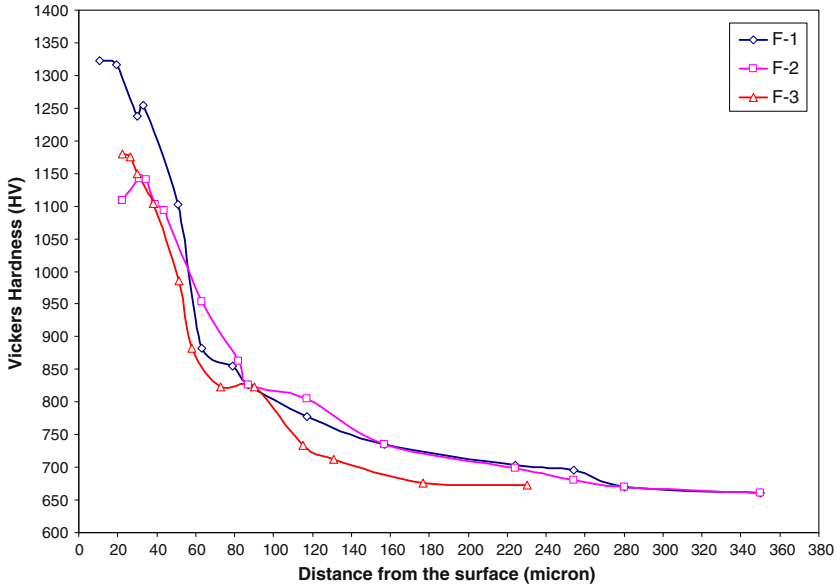

Fig. 6 Hardness-depth profiles for flat features

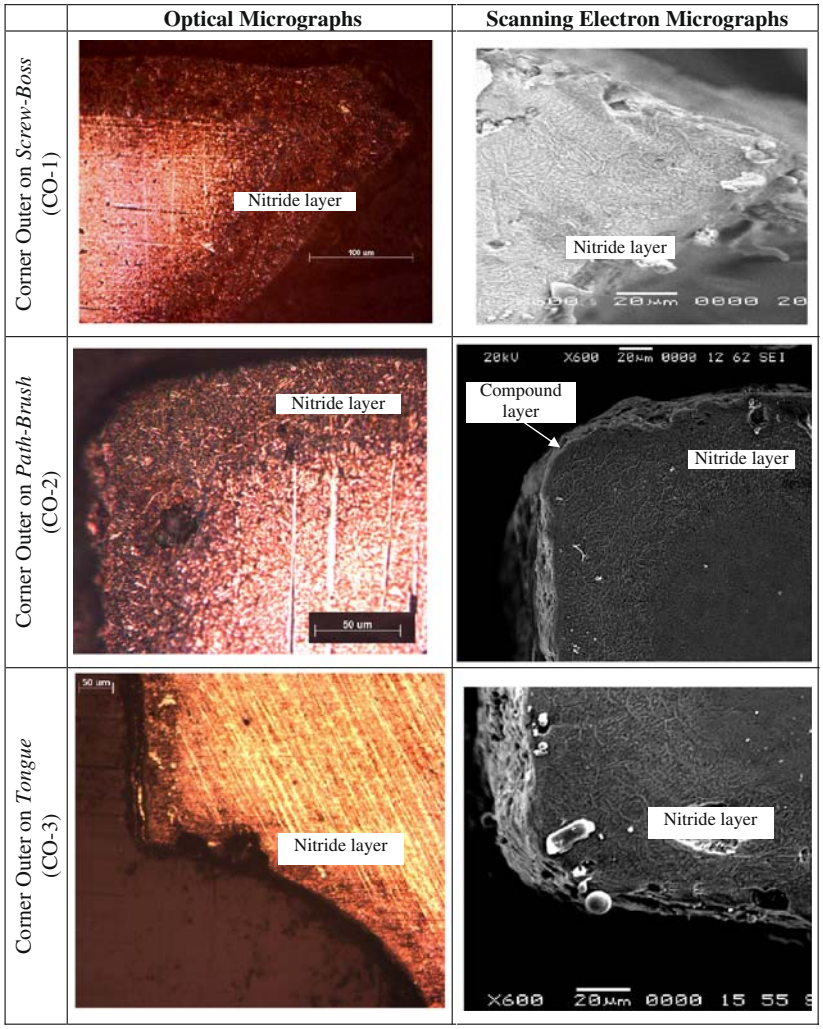

Fig. 7 Optical and scanning electron micrographs of nitrided cross sections observed at corner-outer features

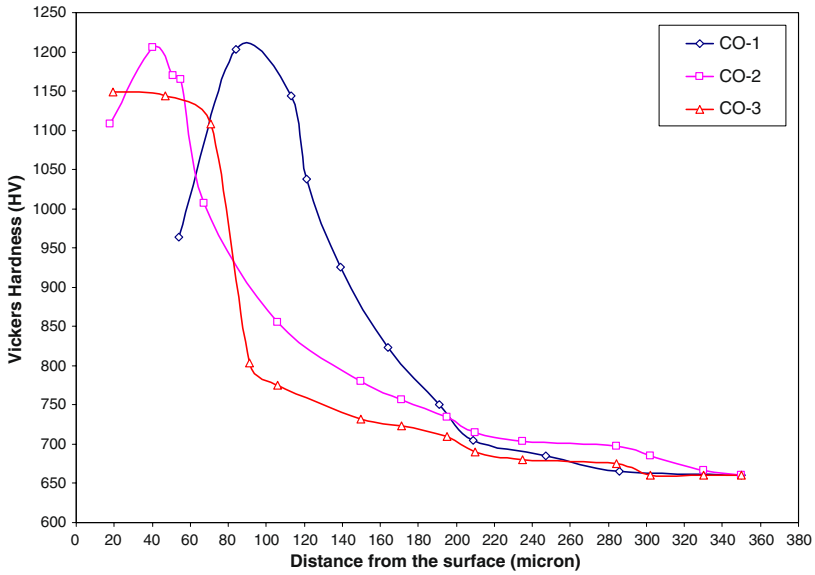

Fig. 8 Hardness-depth profiles for corner-outer features

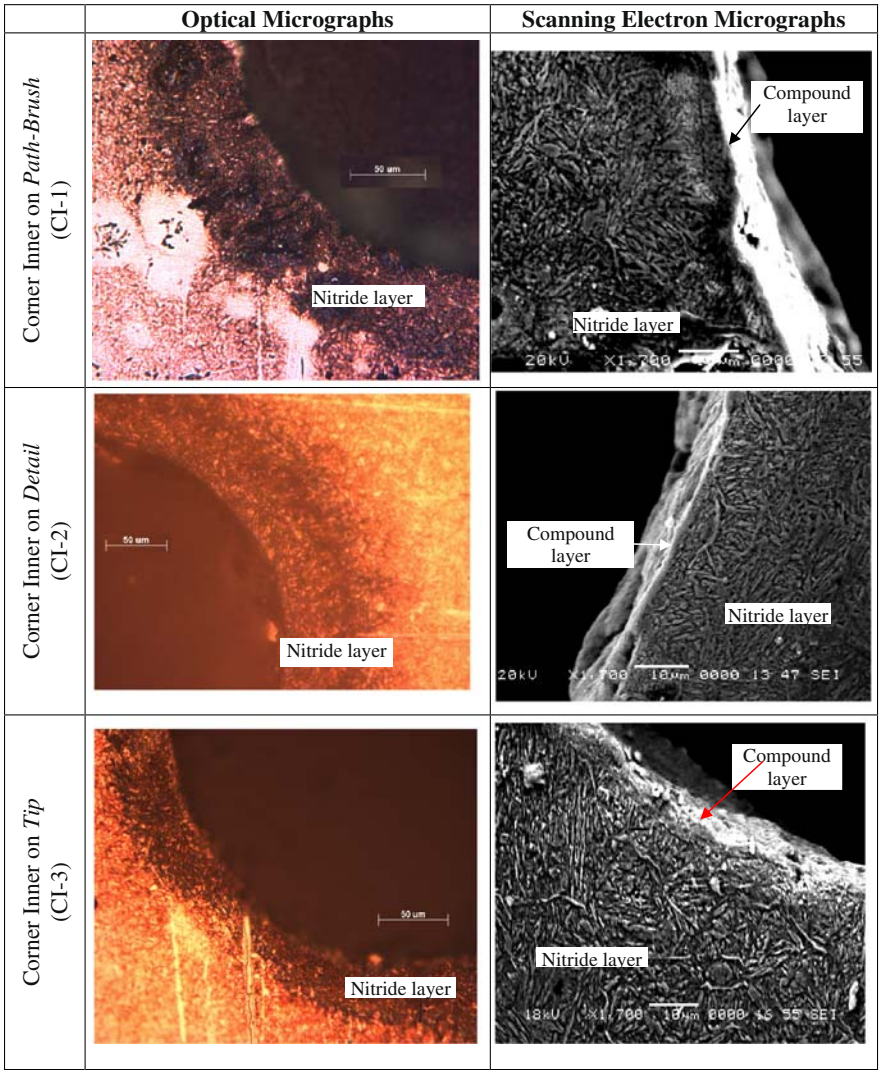

Fig. 9 Optical and scanning electron micrographs of nitrided cross sections observed at corner-inner features

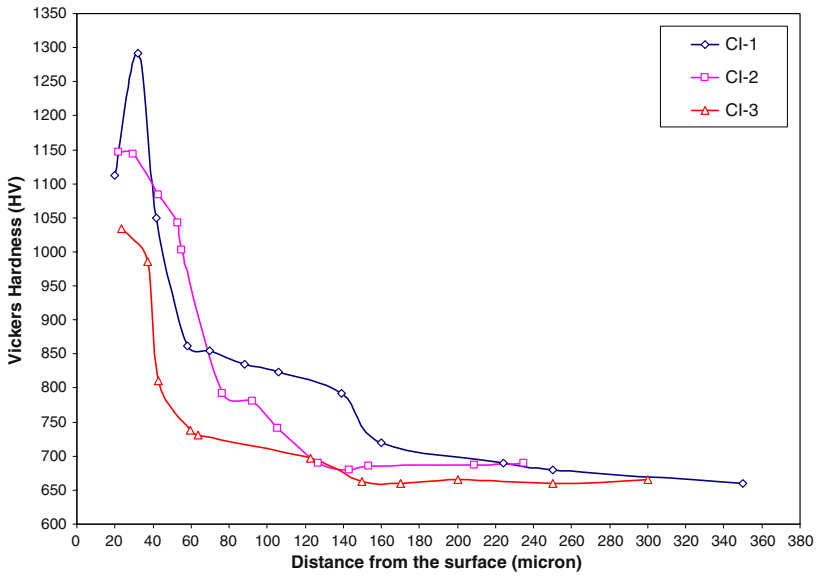

Fig. 10 Hardness-depth profiles for corner-inner features

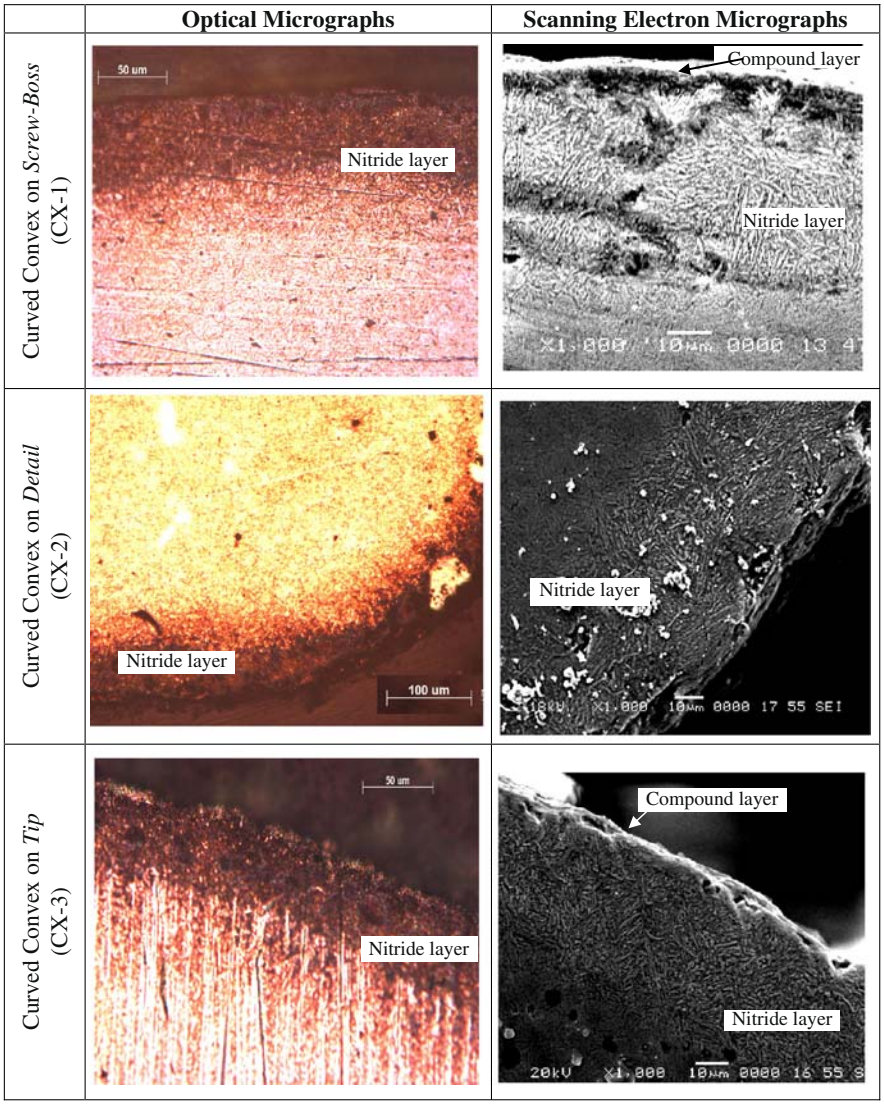

Fig. 11 Optical and scanning electron micrographs of nitrided cross sections observed at curved-convex features

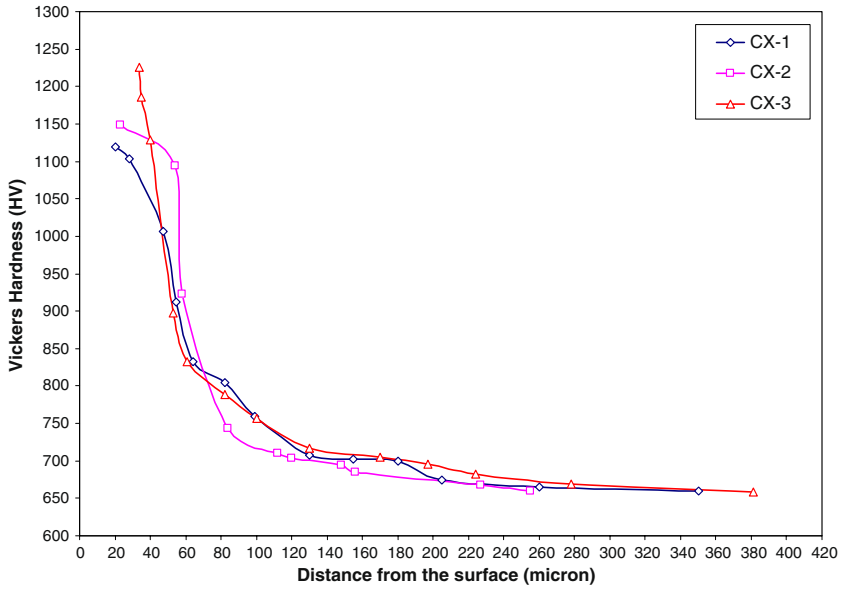

Fig. 12 Hardness-depth profiles for curved-convex features

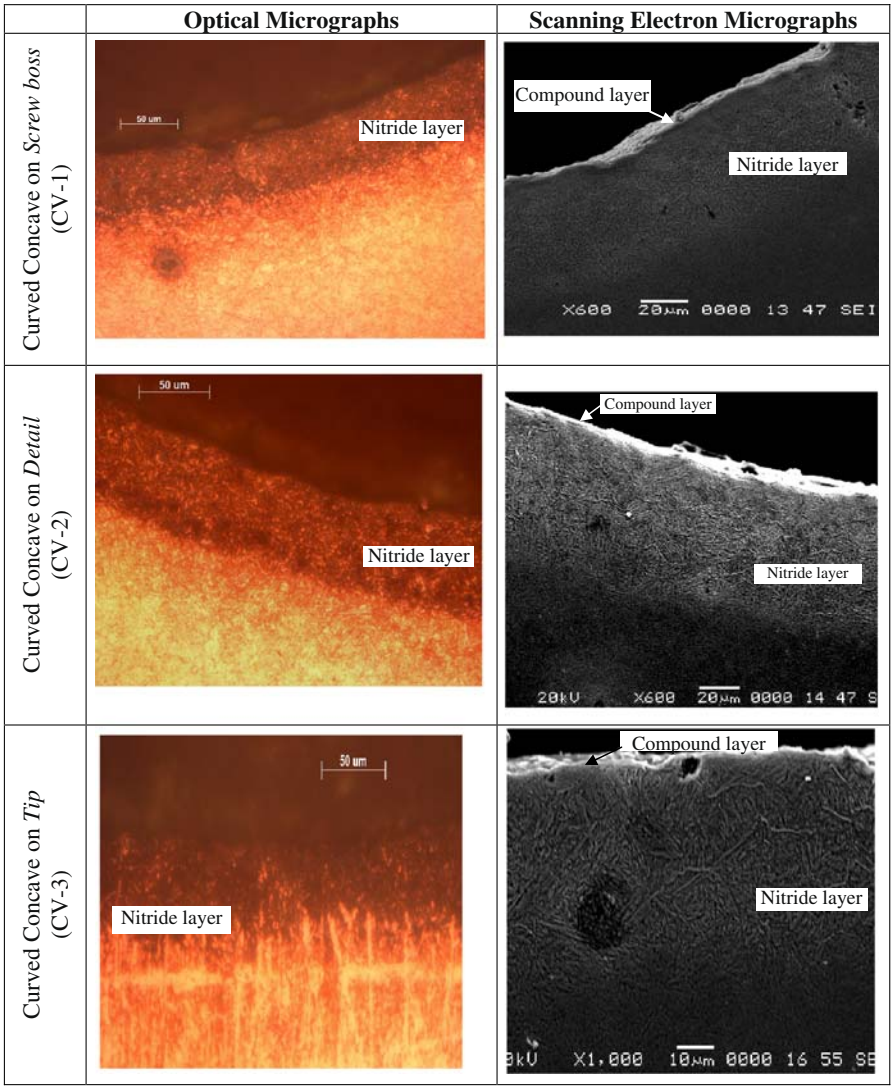

Fig. 13 Optical and scanning electron micrographs of nitrided cross sections observed at curved-concave features

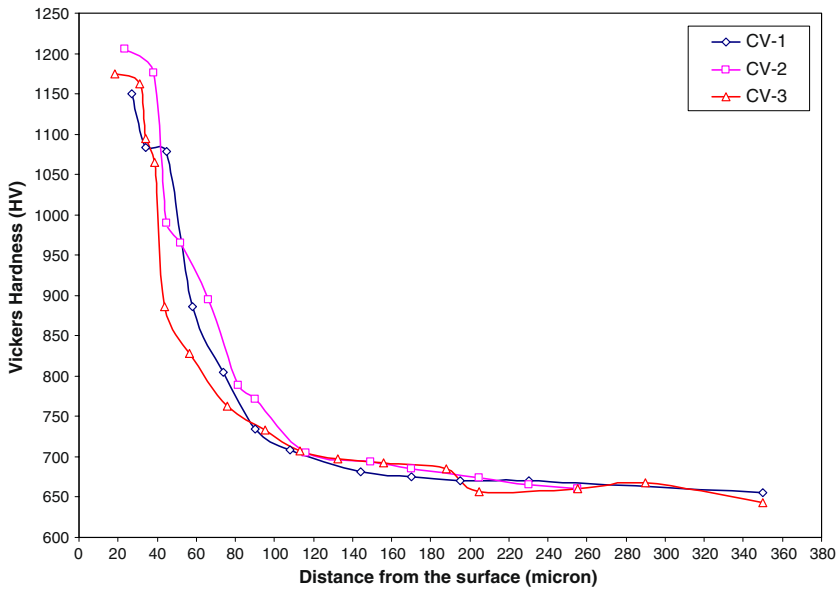

Fig. 14 Hardness-depth profiles for curved-concave features

with greater case depth as compared with other surface profiles. However, oversaturation of nitrogen at the extreme corners resulted in "corner effect", despite the controlled nitriding process. The corner effect results in much reduced initial hardness values resulting from reduced toughness. For instance, in the case of CO-1 (corresponding to screw boss), this effect is significant and a very brittle and spalling nitride layer at the corner is obtained as can be seen from reduced near-surface hardness. As reported by Liliental et al. (Ref 10), many problems experienced with aluminum extrusion dies, the most common including "choke" and "relief" formation occur when debris from such brittle and spalling nitride layer at the corner lodges in the die bearing area. In the case of right-angled outer-corner features, CO-2 and CO-3, this effect is observed to be smaller. In addition to feature itself, the other factor which has an effect on the efficiency of nitriding process and consequent nitrided layer uniformity is the position of feature with regard to the gap and depth. For example, feature CO-3 lies about 15 mm below the exposed surface and the gap available for nitrogen to access this location is only 1 mm as can be observed from the dimensional drawing shown in Fig. 2. Narrow and deep gap significantly affect the nitride layer and the nitride case depth is reduced to 160 μm as compared to the other two corner-outer features, CO-1 and CO-2; in which case, the nitride case depth is 200 μm. Moreover, very steep hardness curve for CO-3 is an indication of reduced load-bearing capacity of the nitrided case.

Table 3 Summary of experimental results

	Experimental measurements	
	Compound layer thickness, μm	Case depth, μm
Geometric feature		
Flat surfaces		
F-1	4-5	170
F-2	3-4	170
F-3	3-4	120
Corner outer		
CO-1	0-5	200
CO-2	0-1	200
CO-3	0-1.5	160
Corner inner		
CI-1	3-4	155
CI-2	3-4	112
CI-3	2-3	75
Curved-convex surface		
CX-1	~5	118
CX-2	0-2	90
CX-3	3-4	120
Curved-concave surface		
CV-1	3-4	100
CV-2	2-3	106
CV-3	2-3	100

3.3 Corner-Inner Feature

They have significantly small case depths particularly for CI-3 as can be observed in Fig. 9. Unlike corner-outer features, simultaneous diffusion from two divergent directions results in reduced nitride case depth at the corner. As compared to flat surfaces, nonuniformity in the nitrided layer can also be observed (Fig. 9). The compound layer developed at these locations is also slightly uneven and its thickness is of the order of 3 μm which is less than that achieved for the flat surfaces. Case depth for CI-3 (corresponding to tip, T-3) is very small and uneven as compared to CI-1 and CI-2. This shows that nitriding does not have a considerable effect on the smaller features. Moreover, the maximum hardness for CI-3 is also small (~1000 HV) as shown in Fig. 10. CI-2 has smaller case depth as compared to CI-1 which is likely due to its acuteness of angle and concealed position. It is worth mentioning here that since all the profiles are cut using wire EDM using about 1 mm diameter wire, a perfect corner is impossible and there

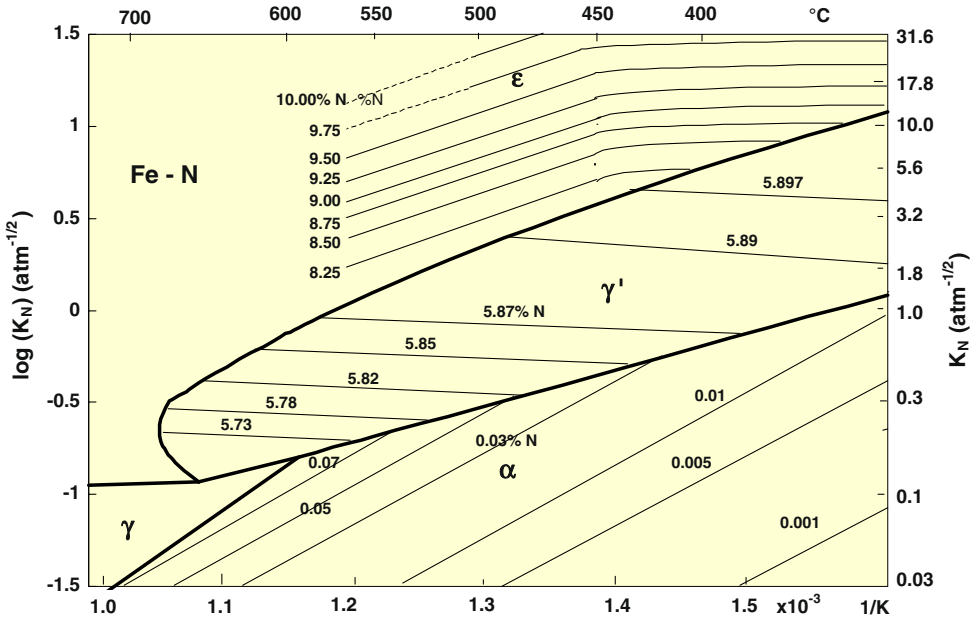

Fig. 15 The Lehrer diagram with adsorption isotherms for iron

must be a fillet of 0.5 mm radius at all corner-inner features. This effect can be seen in the nitrided cross sections.

3.4 Curved-Convex Feature

This has quite uniform nitrided case as well as superficial compound layer except in the case of CX-2 as shown in Fig. 11. The thickness of nitride layer is less than the flat-surface features. However, the compound layer thickness is comparable to that corresponding to the flat-surface features, except in the case of CX-2. A relatively uneven nitride case depth and almost no compound layer at CX-2 can be associated with confined position of the feature leading to inaccessibility of proper nitrogen content during diffusion. The case depth may even be less than the estimated value (90 μm) at some locations of the feature. This observation also confirms the influence of feature position and orientation on the nitriding kinetics. The maximum average hardness is almost the same (about 1150 HV) in all three cases as shown in Fig. 12.

3.5 Curved-Concave Feature

All these features have shown fairly even and uniform nitrided layers as shown in Fig. 13. The observed case depths are relatively shallower than the flat-surfaces. The thickness of compound layer is on the order of 3 μm and found quite uniform as can be observed from the SEM micrographs. The hardness-depth profiles for all the concave positions are almost the same with maximum hardness in the range of 1150 HV comparable with flat locations (Fig. 14).

4. Conclusion

The investigation showed a significant effect of the geometric features on the uniformity, depth and quality of nitrided layer, surface hardness, and hardness profile. The results of this study highlight the need to include the effect of die profile on the nitrided layer for optimal die design with improved service life. Some of the specific conclusions are listed as follows:

- The corner-outer features resulted in deep nitride case depth due to simultaneous diffusion from two convergent directions at the corners. The hardness curves for corner-outer feature locations are relatively less steep and having deeper hardening effect in line with greater case depth as compared to the other surface profiles. However, oversaturation of nitrogen at the extreme corners resulted in "corner effect", despite the controlled nitriding process. The corner effect causes reduced surface hardness values resulting from reduced toughness. The compound layer thickness was the least for these features.
- Unlike corner-outer features, corner-inner features resulted in reduced nitrided case at the corner due to simultaneous diffusion from two divergent directions. It shows that the effect of the angle at which two surfaces meet is critical for the surface hardness and the case depth. The compound layer developed at these locations was slightly uneven and thinner compared to flat-surfaces.
- More uniform compound and nitrided layers were achieved at curved-convex, curved-concave and flat-surface features. The flat-surface features resulted in slightly deeper nitrided case and more uniform and thicker compound layer.
- In general, maximum hardness was observed at locations having curved and flat-surface features.
- In addition to feature itself, its size, location and orientation (with regard to the gap and depth from exposed surface) also play an important part in controlling the nitride case depth size. Large features surfaces showed deeper and more uniform nitrided layers as compared to concealed and small feature surfaces. Narrow and deep gap significantly affected the nitrided layer and resulted in reduced case depth. This can be associated with the availability of the nitrogen access to the locations during diffusion process.

Acknowledgments

The authors acknowledge the support of King Fahd University of Petroleum and Minerals, Dhahran, Saudi Arabia, for the funded project, Project # SB080002 and ALUPCO, Saudi Arabia, for this work.

References

1. S.C. Kwon, M.J. Park, W.S. Baek, and G.H. Lee, Geometric Effect of Ion Nitriding on the Nitride Growth Behavior in Hollow Tube, *J. Mater. Eng. Perform.*, 1992, **1**(3), p 353–358
2. A.R.P. Ataide, C. Alves Jr., V. Hajeka, and J.P. Leiteb, Effects During Plasma Nitriding of Shaped Materials of Different Sizes, *Surf. Coat. Technol.*, 2003, **167**, p 52–58
3. C. Alves Jr., E.F. Silvab da, and A.E. Martinellib, Effect of Workpiece Geometry on the Uniformity of Nitrided Layers, *Surf. Coat. Technol.*, 2001, **139**, p 1–5
4. M. Tercelj, A. Somolej, T. Vecko-Pirtovesek, and R. Turk, The Microstructures and Wear Resistance of Gas-Nitrided and Ionically Nitrided AISI H10 Dies with Narrow Gaps Designed for Hot Extrusion of Aluminum, *JSME Int. J. Ser. C*, 2006, **49**, p 121–127
5. G. Kugler, R. Turk, T. Vecko-Pirtovsek, and M. Tercelj, Wear Behavior of Nitrided Microstructures of AISI H13 Dies for Hot Extrusion of Aluminum, *Metalurgija*, 2006, **45**(1), p 21–29
6. G. Nayal, D.B. Lewisa, M. Lembkea, W.D. Münza, and J.E. Cockremb, Influence of Sample Geometry on the Effect of Pulse Plasma Nitriding of M2 Steel, *Surf. Coat. Technol.*, 1999, **111**(2–3), p 148–157
7. B. Reinhold, J. Naumann, and H.-J. Spies, Influence of Chemical Composition and Geometry on the Nitriding Behavior of Aluminum Alloys, *Harterei-Technische Mitteilungen (Germany)*, 1998, **53**(4), p 329–336
8. Aerospace Material Specification for Automated Gaseous Nitriding Controlled by Nitriding Potential (2579/10A) 2006. http://frontiervalve.com/brochures/amsSpec.pdf
9. A.F.M. Arif, A.K. Sheikh, and S.Z. Qamar, A Study of Die Failure Mechanisms in Aluminum Extrusion, *J. Mater. Process. Technol.*, 2003, **134**(3), p 318–328
10. W.K. Liliental, A. Czelusniak, C.D. Morawski, J. George, and Tymowski, Getting More Life Out of the Aluminum Extrusion Die by Controlled Gas Nitriding, File: T-Tech\TP\PPR\TPAI001.doc, Nitrex Metal Inc., 1999